View metadata, citation and similar papers at core.ac.uk

brought to you by CORE

provided by NASA Technical Reports Server

NASA/TM–2015-217533

Nominal SARAL Transfer Function

David A. Arnold

Frank Lemoine, Editor

July 2015

NASA STI Program ... in Profile

Since its founding, NASA has been dedicated to the advancement of aeronautics and space science. The NASA scientific and technical information (STI) program plays a key part in helping NASA maintain this important role.

The NASA STI program operates under the auspices of the Agency Chief Information Officer. It collects, organizes, provides for archiving, and disseminates NASA's STI. The NASA STI program provides access to the NASA Aeronautics and Space Database and its public interface, the NASA Technical Report Server, thus providing one of the largest collections of aeronautical and space science STI in the world. Results are published in both non-NASA channels and by NASA in the NASA STI Report Series, which includes the following report types:

- TECHNICAL PUBLICATION. Reports of completed research or a major significant phase of research that present the results of NASA Programs and include extensive data or theoretical analysis. Includes compilations of significant scientific and technical data and information deemed to be of continuing reference value. NASA counterpart of peer-reviewed formal professional papers but has less stringent limitations on manuscript length and extent of graphic presentations.
- TECHNICAL MEMORANDUM. Scientific and technical findings that are preliminary or of specialized interest, e.g., quick release reports, working papers, and bibliographies that contain minimal annotation. Does not contain extensive analysis.
- CONTRACTOR REPORT. Scientific and technical findings by NASA-sponsored contractors and grantees.
- CONFERENCE PUBLICATION. Collected papers from scientific and technical conferences, symposia, seminars, or other meetings sponsored or co-sponsored by NASA.
- SPECIAL PUBLICATION. Scientific, technical, or historical information from NASA programs, projects, and missions, often concerned with subjects having substantial public interest.
- TECHNICAL TRANSLATION. English-language translations of foreign scientific and technical material pertinent to NASA's mission.

Specialized services also include organizing and publishing research results, distributing specialized research announcements and feeds, providing help desk and personal search support, and enabling data exchange services. For more information about the NASA STI program, see the following:

- Access the NASA STI program home page at http://www.sti.nasa.gov
- E-mail your question via the Internet to help@sti.nasa.gov
- Fax your question to the NASA STI Help Desk at 443-757-5803
- Phone the NASA STI Help Desk at 443-757-5802
- Write to:

  NASA STI Help Desk
  NASA Center for AeroSpace Information
  7115 Standard Drive
  Hanover, MD 21076-1320

Available from:

NASA Center for AeroSpace Information
7115 Standard Drive
Hanover, MD 21076-1320

National Technical Information Service
5285 Port Royal Road
Springfield, VA 22161

NASA/TM–2015-217533

Nominal SARAL Transfer Function

David A. Arnold
Smithsonian Astrophysical Observatory, Cambridge, MA

Editor:
Frank Lemoine
NASA's Goddard Space Flight Center, Greenbelt, MD

National Aeronautics and
Space Administration

Goddard Space Flight Center
Greenbelt, MD

July 2015

Notice for Copyrighted Information

This manuscript was written by the *Smithsonian Astrophysical Observatory, Cambridge, MA under Grant NNX14AQ52G.* The United States Government has a non-exclusive, irrevocable, worldwide license to prepare derivative works, publish, or reproduce this manuscript, and allow others to do so, for United States Government purposes. Any publisher accepting this manuscript for publication acknowledges that the United States Government retains such a license in any published form of this manuscript. All other rights are retained by the copyright owner.

Trade names and trademarks are used in this report for identification only. Their usage does not constitute an official endorsement, either expressed or implied, by the National Aeronautics and Space Administration.

Level of Review: This material has been technically reviewed by technical management

Nominal SARAL transfer function

by
David A. Arnold
Smithsonian Astrophysical Observatory
60 Garden Street, Cambridge, MA 02138

Abstract

This paper gives a calculation of the range correction and cross section of the SARAL (Satellite with Argos and ALtiKa) Indian/French ocean radar satellite retroreflector array assuming the cube corners are coated and have a dihedral angle offset of about 1.5 arcseconds to account for velocity aberration. The cubes are assumed to all have the same orientation within the mounting. The derived range correction may be applied in precise orbit determination analyses that use Satellite Laser Ranging (SLR) data to SARAL.

Keywords: Satellite laser ranging, Precise orbit determination, SARAL, laser retroreflector array

Table of Contents

1. Introduction

The SARAL spacecraft was launched in February 25, 2013 containing a payload that includes a Ka-Band (35.74 Ghz) ocean radar altimeter. The mission was sponsored by the Indian Space Research Organization (ISRO), and the French Centre Nationale d'Etudes Spatiale (National Space Agency of France). The satellite is destined to operationally map the sea surface from a sun-synchronous orbit, at a mean altitude of ~791 km, and an inclination of 98.54° (Vernon et al., 2015). The orbit is operationally similar to the orbit of the earlier ESA Envisat spacecraft and data from SARAL will fill in the gap in altimeter data coverage between the end of the Envisat mission (~April 2012), and the start of the ESA Sentinel-3 missions (scheduled for launch in late 2015). The laser retroreflector array was developed by the SESO, an optical firm in France (Costes et al., 2010). The purpose of this document is discuss the derivation of range correction for this laser retroreflector array for use in precise orbit determination (POD).

2. Simulations

The document "saral_retro_cnes_201304.pdf" (presented at the ILRS Analysis Working Group Meeting, Technical University of Vienna, April 7, 2013; http://ilrs.gsfc.nasa.gov/science/awg/awgActivities/index.html), gives details of the construction of the array. The data on slide 4, "Correction to the optical center ", shown below is used to calculate the geometry of the array. (This presentation is an extract of the CNES SARAL document from Noubel (2013)).

Correction to the optical center

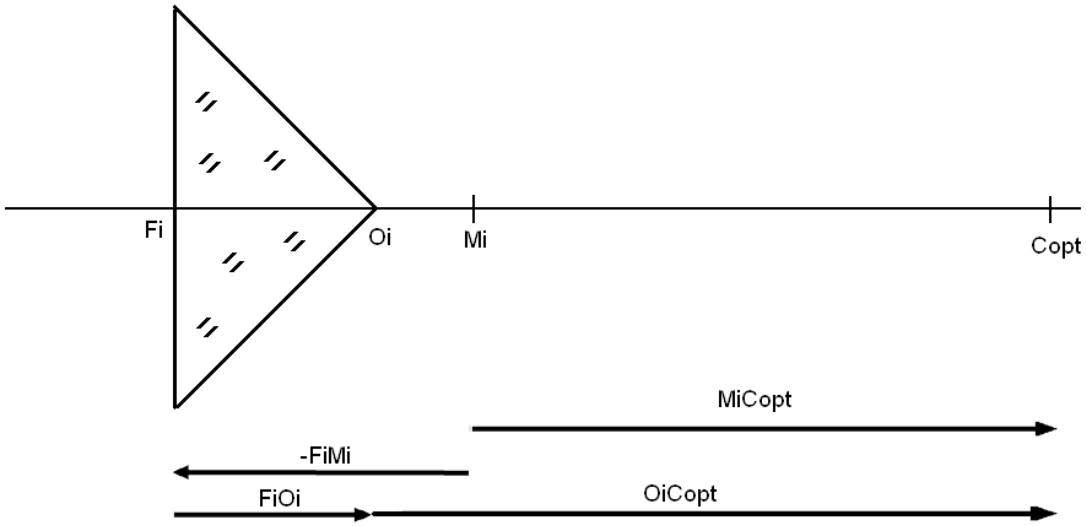

FiOi = 24.3 ± 0.1 mm, except for corner cube 8: 24.45 mm
FiMi = 35.5 ± 0.1 mm, except for corner cube 8: 35.72 mm
OiC_{opt} = 55.0 ± 0.1mm, except for corner cube 8: 54.6 mm
MiC_{opt} = 43.8 ± 0.1 mm, except for corner cube 8: 43.4 mm

Figure 1. Correction to the optical center of the array.

The length of the cube corners is L = FiOi = 24.3 mm. Since the front face is $L\sqrt{2}$ the diameter of the front face is 34.36 mm = 1.35 inches. The distance from the front face to the optical center of the array is FiOi + OiC_{opt} = 24.3 + 55.0 = 79.3 mm = .0793 meters.

These quantities have been used to compute coordinates of the 9 cube corners as shown in Table 1 below. The Z axis points from the optical center of the array to the center of the front face of the pole cube. The X axis points in the direction of the first cube in the ring of 8. The range correction will be computed relative to the optical center of the array. This can be related to the center of gravity of the spacecraft.

Row	Unit	X(m)	Y(m)	Z(m)	Theta (deg)	Phi (deg)
1	1	0.00000	0.00000	0.07930	0.000	0.000
2	1	0.06075	0.00000	0.05097	0.000	50.000
2	2	0.04295	0.04295	0.05097	45.000	50.000
2	3	0.00000	0.06075	0.05097	90.000	50.000
2	4	-0.04295	0.04295	0.05097	135.000	50.000
2	5	-0.06075	0.00000	0.05097	180.000	50.000
2	6	-0.04295	-0.04295	0.05097	225.000	50.000
2	7	0.00000	-0.06075	0.05097	270.000	50.000
2	8	0.04295	-0.04295	0.05097	315.000	50.000

Table 1. Position and orientation of the cubes in the array. Phi is measured from the Z axis. Theta is measured from the X axis toward the Y axis. Row 2 is the ring of 8.

Two simulations have been done using the method described in Reference 3. The first gives the range correction and cross section for Phi = 0 to 50 deg at 5 deg intervals at Theta = 0. This is moving toward the first cube corner in the ring of 8. The second calculation is for Phi = 0 to 50 deg at Theta = 22.5 deg. The is moving toward the space between cubes 1 and 2 in the ring of 8. The results are shown in the next two tables.

Incidence angle Phi (deg)	Range Corr (m)	Cross Section (million sq m)
0.000	0.040308	1.189484
5.000	0.039359	1.111924
10.000	0.037644	1.077196
15.000	0.036183	1.045180
20.000	0.035435	1.039058
25.000	0.035372	1.055090
30.000	0.036047	1.086151
35.000	0.037236	1.144655
40.000	0.038498	1.244323
45.000	0.039592	1.329218
50.000	0.040286	1.403162
55.000	0.040010	1.232458
60.000	0.039051	1.046831
65.000	0.037539	0.848495
70.000	0.035907	0.647337
75.000	0.034133	0.440475
80.000	0.032378	0.260382
85.000	0.030721	0.153421
90.000	0.028185	0.098429

Table 2. Range Correction and cross section for Phi = 0° to 90° at Theta = 0°. The values are the average over the 25 to 50 microradian annulus in the far field.

Incidence angle Phi (deg)	Range Corr (m)	Cross Section (million sq m)
0.000	0.040308	1.189484
5.000	0.039357	1.114473
10.000	0.037618	1.075704
15.000	0.036134	1.044136
20.000	0.035225	1.041072
25.000	0.035043	1.074128
30.000	0.035693	1.120982
35.000	0.036812	1.184699
40.000	0.037884	1.239935
45.000	0.038764	1.248189
50.000	0.039482	1.190520
55.000	0.039618	1.113131
60.000	0.038980	1.002068
65.000	0.037723	0.835650
70.000	0.035930	0.634961
75.000	0.033688	0.448836
80.000	0.031013	0.312559
85.000	0.027916	0.207859
90.000	0.024408	0.112804

Table 3. Range Correction and cross section for Phi = 0° to 90° deg at Theta = 22.5°. The values are the average over the 25 to 50 microradian annulus in the far field

The range correction and cross section vs. incidence angle are shown in Figures 2 and 3, shown below.

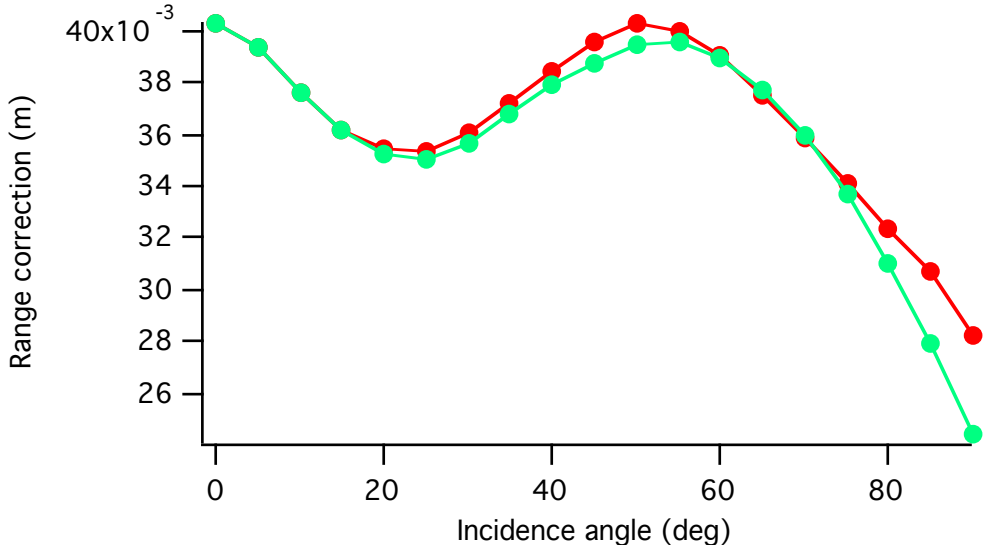

Figure 2. Range correction (m) for Phi = 0° to 90°. The red curve is for Theta = 0° and the green is for Theta = 22.5°. The range correction differs by .8 mm at incidence angle 50°. The minimum range correction at 25° is lower by about 5 mm.

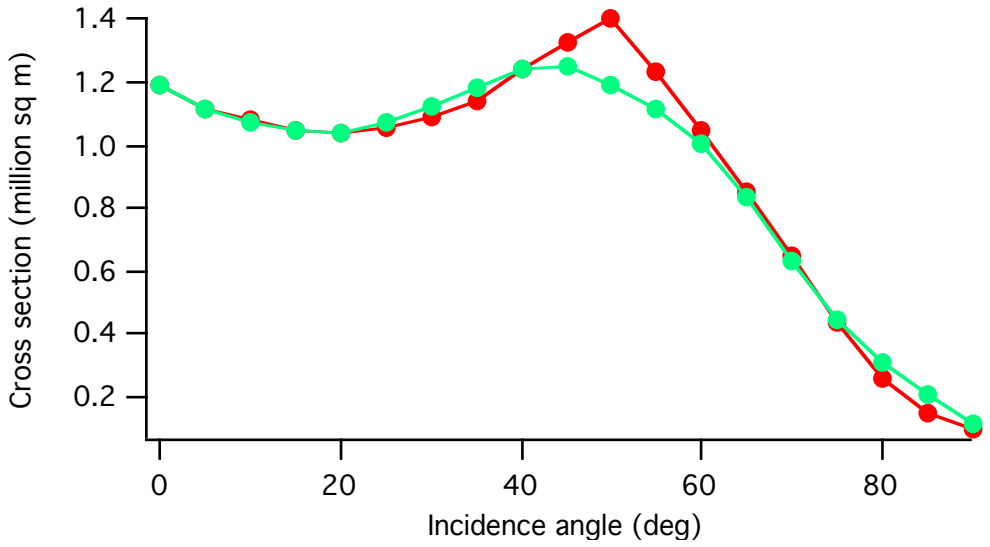

Figure 3. Cross section (million sq m) for Phi = 0° to 90°. The red curve is for Theta = 0° and the green is for Theta = 22.5°. The cross section for 22.5° is lower by 0.2 million sq m at 50° incidence angle.

3. Alternative method of calculation.

The transfer function can be computed in various ways. The primary way is to add the diffraction patterns of all active reflectors to get the total cross section matrix and compute the weighted mean position of the return from the active cube corners at each point in the far field diffraction pattern. The average value of the cross section and range correction within the velocity aberration annulus can computed from these matrices. This is the way Tables 2 and 3 were computed.

An alternative approach is to compute the average cross section of each active cube corner within the velocity aberration annulus and then use this average value to compute the total cross section and weighted mean position of the return signal. The average cross section in the velocity aberration annulus and apparent reflection point are computed and recorded during the calculation of the cross section and range correction matrices for the whole array. Using the average cross section for each cube to compute the range correction gives the same answer as the first method to within the accuracy of the averaging of the matrices.

Table 4 below shows the contribution of each active cube corner at normal incidence on the array from Table 2.

ROW	UNIT	POSITION (m)	CROSS SECTION (million sq m)
1	1	0.043239	1.060199
2	1	0.020085	0.016144
2	2	0.020085	0.016177
2	3	0.020085	0.016144
2	4	0.020085	0.016177
2	5	0.020085	0.016144
2	6	0.020085	0.016177
2	7	0.020085	0.016144
2	8	0.020085	0.016177

Table 4. Position of the effective reflection point and cross section of each active cube corner in the array at Phi = 0° and Theta = 0°.

The data in Table 4 can be used to compute the range correction. The cross section of the cubes in the ring of 8 is .0161 x 8 = .1292. The total cross section is 1.0602 + .1292 = 1.1912. This is in good agreement with the first entry in Table 2. The range correction ΔR is the average position of the active cubes weighted by the cross section. From the values in Table 4 we have

ΔR = (1.0602 x .0432 + .1292 x .0201)/1.1912 = (.0458 + .0026)/1.1912 = .0406 m

ΔR minus the first entry in Table 2 is .0406 - .0403 = .3 mm which is good agreement between the two different ways of computing the range correction.

4. Position of the closest cube vs range correction.

For this array using only the range correction for the closest cube gives a value that is close to the full calculation. The difference Δ ranges from 1 to 3 mm. This can be useful for doing back-of-the-envelope calculations for this type of array. The optical path length within a cube corner is given on page 8 of SAO Special Report 382 as

$$OPL = L\sqrt{n^2 - \sin^2 i} \qquad (1)$$

where *OPL* is the optical path length, *n* is the index of refraction, *L* is the length of the cube corner, and *i* is the angle of incidence on the cube corner. Equation (1) can be used to compute the optical path length and effective reflection point for the closest cube corner for the cases that have been studied. Two examples are given below.

1. At Phi = 0° the incident beam is normal to the pole cube. The range correction for the cube corner is $\Delta R = R - nL$ where R = .0793 m is the optical radius of the array, n is the group index of refraction and L is the length of the cube corner. The optical path length in the cube corner is nL = 1.484 x .0243 = .0363 m. The range correction for the first cube is ΔR = .0793 - .0363 = .0432 m in agreement with the first entry in Table 4. The range correction from Table 2 for Phi = 0 is .0403 m. If we define Δ as the position of the closest cube minus the range correction we have Δ = .0432 - .0403 = 3 mm. This is a fairly small difference.

2. At Phi = 25 deg the incident beam is halfway between the pole cube and the ring of 8. The front face of the closest cubes is $R\cos(25)$ = .0718 m from the optical center. The optical path length in the cube corner from equation (1) with n = 1.484 and i = 25 deg is *OPL* = .0345 m. The range correction for the closest cubes is ΔR .0718 - .0345 = .0373 m in agreement with the first entry in Table 5 below. The range correction from Table 2 for Phi = 25 deg is .03537. The position of the closest cube minus the range correction is Δ = .0373 - .03537 = 2 mm. This is a small difference.

ROW	UNIT	POSITION (m)	CROSS SECTION (million sq m)
1	1	0.037302	0.353639
2	1	0.037300	0.391777
2	2	0.031198	0.152366
2	3	0.016023	0.002470
2	7	0.016023	0.002470
2	8	0.031198	0.152368

Table 5. Position of the effective reflection point and cross section of each active cube corner in the array at Phi = 25° and Theta = 0°.

The only cubes having significant cross section are the pole cube (1,1), the first cube (2,1) in the ring of 8 and cubes (2,2) and (2,8) on either side of the first cube in the ring. Cubes (2,3) and (2,7) have negligible cross section. The incidence angle on the first two cubes in Table 5 is 25 degrees. They do not have exactly the same cross section because the cross section depends on both the angle Phi from the normal to the front face and the angle Theta about the normal. At constant Phi the cross section vs Theta repeats every 120 deg if all the dihedral angle offsets are identical.

ROW	UNIT	POSITION	CROSS SECTION
		(m)	(million sq m)
1	1	0.020088	0.017034
2	1	0.043239	1.060134
2	2	0.032275	0.162996
2	8	0.032275	0.162998

Table 6. Position of the effective reflection point and cross section of each active cube corner in the array at Phi = 50° and Theta = 0°.

The first cube (2,1) in the ring of 8 is at normal incidence. The adjacent cubes (2,2) and (2,8) in the ring are the only other cubes having significant cross section. The pole cube (1,1) has negligible cross section. The position of the closest cube minus the range correction at Phi = 50 deg from Table 2 is Δ = .04324 - .04028 = 3 mm.

ROW	UNIT	POSITION	CROSS SECTION
		(m)	(million sq m)
1	1	0.037302	0.367585
2	1	0.035724	0.298880
2	2	0.035721	0.298878
2	3	0.024324	0.054392
2	8	0.024322	0.054394

Table 7. Position of the effective reflection point and cross section of each active cube corner in the array at Phi = 25° and Theta = 22.5°.

The only cubes with large cross section are the pole cube (1,1) and the first two cubes (2,1) and (2,2) in the ring of 8. The position of the closest cube (1,1) minus the range correction for Phi = 25° in Table 3 is Δ = .0373 - .0350 = 2 mm.

ROW	UNIT	POSITION	CROSS SECTION
		(m)	(million sq m)
1	1	0.020088	0.016281
2	1	0.040419	0.572617
2	2	0.040412	0.572615
2	3	0.019748	0.014502
2	8	0.019745	0.014503

Table 8. Position of the effective reflection point and cross section of each active cube corner in the array at Phi = 50° and Theta = 22.5°.

The only cubes with significant cross section are the first two cubes (2,1) and (2,2) in the ring of 8. The position of the closest cubes minus the range correction for Phi = 50 deg from Table 3 is Δ = .04041 - .03948 = 1 mm. The table below summarizes the difference Δ = position of closest cube - range correction.

Theta (deg)	0	0	0	22.5	22.5
Phi (deg)	0	25	50	25	50
Δ (mm)	3	2	3	2	1

Table 9. Difference Δ between the position of the closest cube and the range correction.

5. Summary

In Table 2 the range correction has a maximum value of .0403 m at Phi = 0° and 50° incidence angle. It decreases by 5 mm and reaches a minimum of .0353 m at around Phi = 25°. From Figure 1 we see that it is not very sensitive to the azimuth (Theta) of the incidence beam. The cross section (Figure 2) is about 1.2 million sq m at normal incidence, has a minimum of about one million sq m at 20 degrees incidence angle, and is 1.2 to 1.4 million sq m at 50 degrees. Section 3 shows that the difference Δ between the position of the closest cube and the range correction is from 1 to 3 mm. This makes it possible to calculate the range correction to reasonable accuracy by hand.

6. Conclusions

The fact that the range correction is not very different from the range to the closest cube means that the range correction should be nearly the same for different types of ranging systems. This is a sparse array. There is a separation of 45 degrees or more between cube corners. The bulk of the return comes from a small number of cubes that are close in range. Because it is a sparse array there is a variation in the range correction with incidence angle. This differs from spherical satellites with a large number of cubes where the return is largely independent of the orientation of the satellite. The range correction is largest when the incident beam is normal to one of the cubes and smallest when the incident beam is between cubes. If the satellite is 3-axis stabilized so that the orientation of the array is known it would be possible to apply a range correction as a function of the incidence angle on the array.

7. References

Arnold D.A., (1979). Method of Calculating Retroreflector-Array Transfer Functions, Smithsonian Astrophysical Observatory Special Report No. 382, 165 pp. http://ilrs.gsfc.nasa.gov/docs/1979/1979SAOSR_382.pdf

Costes V., Karine Gasc K, Sengenes P., et al. (2010). Development of the Laser Retroreflector Array (LRA) For Saral, International Conference on Space Optics, proceedings paper, October 4-8 2010, Rhodes, Greece.

Noubel J. (2013). SARAL characteristics For DORIS calibration plan And POD Processing, CNES document SRL-SYS-NT-066-CNES revision 2, May 5 2013 (ftp://ftp.ids-doris.org/pub/ids/satellites/Saral_CharacteristicsForDORISCalibrationPlanAndPODProcessing.pdf).

Vernon J., Sengenes P., Lambin J., et al. (2015). The SARAL/AltiKa Altimetry Satellite Mission, *Marine Geodesy*, doi: 10.1080/01490419.2014.1000471.